Available online at www.sciencedirect.com
ScienceDirect
Scripta Materialia 65 (2011) 171–174
Scripta MATERIALIA
www.elsevier.com/locate/scriptamat

Homogeneity of ultrafine-grained copper deformed by high-pressure torsion characterized by positron annihilation and microhardness

J. Čížek,[a,*] O. Melikhova,[a] M. Janeček,[a] O. Srba,[a] Z. Barnovská,[a] I. Procházka[a] and S. Dobatkin[b]

[a] *Faculty of Mathematics and Physics, Charles University in Prague, V Holešovičkách 2, Prague 8, CZ-18000, Czech Republic*
[b] *A.A. Baikov Institute of Metallurgy and Materials Science, Russian Academy of Sciences, Moscow, Russia*

Received 22 February 2011; revised 1 April 2011; accepted 7 April 2011
Available online 12 April 2011

Spatially resolved positron annihilation was employed for mapping lateral defect distribution in Cu deformed by high-pressure torsion. Parameters describing Doppler broadening of the annihilation peak were used for mapping the spatial distribution of defects. In comparison with microhardness showing a clear development towards homogeneity, positron annihilation revealed that spatial distribution of defects was far from uniform, even after 25 turns. This was mainly due to a higher concentration of deformation-induced vacancies at the periphery compared with the center.

Keywords: Severe plastic deformation; High-pressure torsion; Lattice defects; Vacancies; Positron annihilation

High-pressure torsion (HPT) is a well-established technique based on severe plastic deformation (SPD), which causes significant grain size refinement and enables bulk ultrafine-grained (UFG) materials with sub-micrometer grain size to be produced [1]. In HPT processing, a disk-shaped sample located between two anvils is subjected to a compressive pressure of several gigapascals and simultaneously strained by a rotating anvil. Hence, the applied compressive pressure p and the number of rotations N are the most important parameters in HPT processing. The shear strain γ imposed on the disk during HPT processing can be estimated from the relationship [1]

$$\gamma = \frac{2\pi N r}{h}. \quad (1)$$

Here, N is the number of HPT revolutions, h denotes thickness of the deformed sample, and r is the sample radius. For a disk-shaped sample, the imposed strain increases with the radial distance r from zero in the disk center (corresponding to the rotation axis) up to a maximum value at the edge. Hence, one can expect that the microstructure varies across the sample, owing to inhomogeneous strain. Indeed, TEM investigations of HPT-deformed Cu [2,3] and Ni [4] revealed coarser microstructure in the centre compared with the periphery.

Vicker's microhardness (HV) testing proved to be a very useful technique for characterization of the homogeneity of HPT-deformed samples. Detailed HV characterizations of HPT-deformed Ni [4] revealed a lower HV in the center and a higher HV at the periphery. With increasing number of HPT turns, HV in the center increases, and the difference between the center and the periphery thereby decreases and finally diminishes after a sufficient number of rotations. Similar results were obtained also on HPT-deformed Cu [3] and technical purity Al [5]. The microstructure evolution of HPT-deformed samples and its gradual development towards homogeneity has been successfully modeled using strain gradient plasticity theory [6]. Recent HV characterizations of HPT-deformed high-purity Al [7,8] revealed dynamic recovery of the UFG structure, starting in the most strained region at the periphery. This effect leads to a softening, i.e., HV at the periphery becomes lower compared with the center [7,8]. Hence, there is a significant difference in the microstructure across the sample disk in materials such as high-purity Al, where dynamic recovery occurs during HPT processing, and other materials where this effect is absent. Nevertheless, the general trend in all samples is a diminishing difference between

* Corresponding author. Tel.: +420221912788; fax: +420221912567; e-mail address: jakub.cizek@mff.cuni.cz

1359-6462/$ - see front matter © 2011 Acta Materialia Inc. Published by Elsevier Ltd. All rights reserved.
doi:10.1016/j.scriptamat.2011.04.006

the center and the periphery with increasing number of rotations [3–8]. Recently, it was shown that new HPT techniques capable of producing massive specimens with diameters in the centimeter range produce samples with almost homogeneous UFG microstructure [9].

Inhomogeneities of the shear strain in HPT processing result obviously in inhomogeneous lateral distribution of deformation-induced defects. This effect was investigated in the present work by employing positron annihilation spectroscopy [10], which is a well-established non-destructive technique with high sensitivity to open-volume defects. Previous positron lifetime (LT) investigations of HPT-deformed Cu revealed two types of open-volume defects [3]: (i) dislocations; and (ii) small vacancy clusters. Moreover, it was found that the size of vacancy clusters increases with the radial distance from the center, and the concentration of deformation-induced vacancies increases with increasing number of HPT revolutions [3].

In this work, the Doppler broadening (DB) technique [10] was employed for mapping of the lateral defect distribution in HPT-deformed Cu. A non-zero momentum of annihilating electron–positron pairs leads to a Doppler shift in energy of annihilation radiation. Since the momentum of the thermalized positron is negligible compared with that of the electron, the Doppler shift carries information about the one-dimensional momentum distribution of the electrons. The Doppler shift causes broadening of the annihilation photopeak in the γ-ray energy spectrum, which can be precisely quantified using so-called line-shape parameters S and W [10]. The S parameter, defined as the central area of the annihilation peak divided by the net peak area, is a measure of the contribution of positrons annihilated by low-momentum electrons. The W parameter, defined as the area under "wings" of the annihilation peak divided again by the net peak area, is a measure of the contribution of positrons annihilated by high-momentum electrons. When a positron is trapped at an open volume defect, its wave function becomes localized in the defect, which leads to a reduction of its overlap with high-momentum core electrons. As a consequence, the S parameter increases, while W decreases. Hence, line-shape parameters can be used for mapping the spatial distribution of defects across the sample. The main advantage of the DB technique is that it is relatively fast. While measurement of the LT spectrum with sufficient statistics of 10^7 annihilation events takes at least 1 day using a standard positron source with activity 1.5 MBq, in the DB technique it is sufficient to measure ~30 min to obtain reliable line-shape parameters. This makes it feasible to use the DB technique for mapping of the lateral distribution of defects in HPT-deformed samples.

Technical purity Cu (99.95 wt.%) specimens were subjected to room temperature quasi-constrained HPT straining using a compressive pressure of 4 GPa. HPT-deformed specimens were disk shaped, with diameter ~9 mm and thickness ~0.5 mm. Samples subjected to 1, 3, 5, 10, 15 and 25 HPT revolutions were investigated.

The homogeneity of the microstructure was characterized by HV measurements on a perpendicular grid with incremental spacing of 0.5 mm, performed using a STRUERS Duramin 300 hardness tester with load of 100 g applied for 10 s. Color-coded maps of the HV results were constructed to provide pictorial displays of the homogeneity of the microstructure across the sample.

DB measurements were performed using a $^{22}Na_2CO_3$ positron source with activity ~0.5 MBq. The source spot was carefully deposited on 2 μm mylar foil so that the spot diameter was smaller than 1 mm. The mean penetration depth of positrons emitted by the ^{22}Na source into Cu was ~30 μm. The energy of the annihilation photons was measured by a high-purity germanium (HPGe) detector with energy resolution 1.30 keV at 511 keV. Pulses from the HPGe detector were processed in a spectroscopic track consisting of a spectroscopy amplifier and an analogue-to-digital converter. The central region for calculation of the S parameter was chosen symmetrically around the 511 keV annihilation peak from 510.16 to 511.84 keV. Energy ranges of 504.00–507.43 keV and 514.57–518.00 keV on tails of the annihilation peak were used for calculation of the W parameter. All S values presented in this work were normalized to the S parameter $S_0 = 0.5045(5)$ measured in the centre of the Cu sample subjected to one HPT revolution. Similarly, W parameters were normalized to $W_0 = 0.02991(1)$. DB measurements were performed on a perpendicular grid with incremental spacing of 1.0 mm by placing the positron source spot at various nodes of the grid using a micrometer x–y shift. The uncertainty in position of the positron source was ~0.1 mm. Similarly to the HV measurements, DB results were also plotted in color-coded maps.

Color-coded maps showing the HV distribution over a Cu sample subjected to 1 and 25 HPT revolutions, respectively, are plotted in Figure 1a and c. As expected, the spatial distribution of HV retains radial symmetry. The sample subjected to one HPT revolution exhibits a lowered HV of ~116 in the center, while the periphery

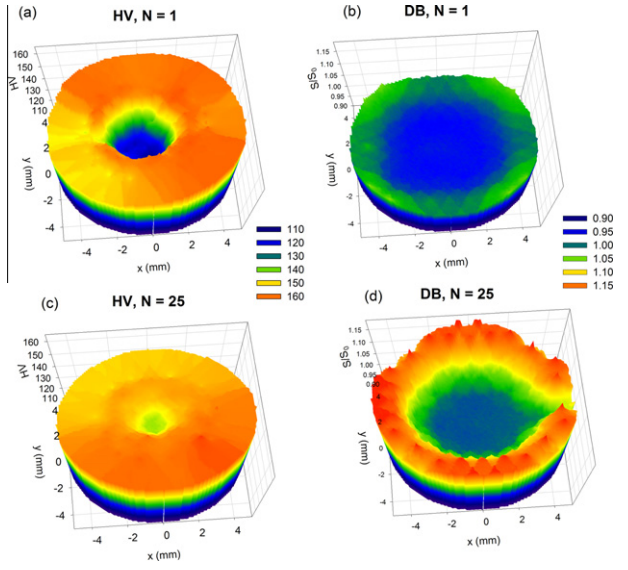

Figure 1. Color-coded map constructed from (a) HV values and (b) S parameter determined by DB on a perpendicular grid in Cu sample subjected to 1 HPT revolution; (c) HV values; (d) S parameter mapping in sample subjected to 25 HPT turns.

is characterized by a high HV of ~150. With increasing number of HPT revolutions, the HV in the center increases, and the difference between the center and the periphery becomes smaller. Obviously, high HV at the periphery already after the first HPT revolution is caused by the fact that this region is subjected to the highest strain. With increasing number of HPT turns, the region characterized by high HV extends gradually towards the center. The sample subjected to 25 HPT turns exhibits almost uniform HV everywhere at $r > 1$ mm. However, the center is still characterized by slightly lower HV. Note that this behavior is in accordance with previous HV investigations of HPT-deformed Cu [2] and Ni [4] as well as with strain gradient modeling [6].

Mapping of the lateral defect distribution by the DB technique was performed on Cu samples subjected to 1, 3, 15 and 25 HPT turns. Color-coded maps of the S parameter measured on the sample subjected to 1 and 25 HPT turns, respectively, are shown in Figure 1b and d. The dependence of the S and the W parameters on the radial distance r from the center of the sample disk is plotted Figure 2. The S parameter increases with the radial distance from the center, while the W parameter decreases. LT investigations of HPT-deformed Cu samples revealed that positrons annihilate from the trapped state either at dislocations or in small vacancy clusters [3]. Note that trapping at grain boundaries can be neglected because positrons are trapped at distorted layers with high dislocation density surrounding grain boundaries [3]. Hence the S parameter measured in HPT-deformed Cu samples can be written as

$$S = S_d(1 - F_{vc}) + S_{vc}F_{vc}, \quad (2)$$

where F_{vc} is the fraction of positrons annihilated from the trapped state in vacancy clusters, and S_d, S_{vc} denote the S parameter for positrons trapped at dislocations and in vacancy clusters, respectively. Analogous with Eq. (2), the W parameter can be expressed as:

$$W = W_d(1 - F_{vc}) + W_{vc}F_{vc}, \quad (3)$$

where W_d and W_{vc} denote the W parameter for positrons trapped in dislocations and in vacancy clusters, respectively. Note that $S_{vc} > S_d$, while $W_{vc} < W_d$, because vacancy clusters contain more open space than dislocations. X-ray diffraction line profile analysis revealed that dislocation density at the periphery is virtually the same as in the center, i.e., there is only a slight variation in dislocation density across the sample. However, the size of vacancy clusters in the center corresponds to about five vacancies, while vacancy clusters at the periphery are bigger and consist on average of eight vacancies [3]. Vacancy clusters were formed by agglomeration of deformation-induced vacancies. The larger size of vacancy clusters at the periphery is therefore caused by the higher strain imposed in that region. Since bigger clusters exhibit larger cross sections for positron trapping, the fraction F_{vc} is higher at the periphery than in the center [3]. The increasing fraction of positrons annihilating in vacancy clusters together with increasing cluster size lead to a strong increase in the S parameter with the radial distance from the center accompanied by a decrease in the W parameter. The concentration of vacancy clusters increases with increasing number of HPT revolutions, owing to additional vacancies introduced into the sample. This is reflected by an overall increase in S (Fig. 2a) and corresponding decrease in W (Fig. 2b) with increasing number of HPT revolutions. Figure 1 testifies that spatial distribution of defects in HPT-deformed samples retains radial symmetry. A significant change in defect distribution reflected by a substantial rise in S at the periphery occurs in the sample subjected to three HPT turns. In comparison with the sample subjected to one HPT revolution, the concentration of vacancy clusters both in the center and at the periphery increases with increasing number of HPT revolutions, which was confirmed also by LT investigations [3].

The dependence of W on S (the so-called S–W plot) is shown in Figure 3. If the nature of positron traps does not change (i.e., the S and W parameters characteristic for dislocations and vacancy clusters do not change) and only the concentration of defects varies, a linear relationship between S and W can be derived from Eqs. (2) and (3). Under such conditions S, W values measured in various positions in the sample fall on a line connecting a point characteristic for one type of defect (here the point $[S_d, W_d]$ representing dislocations) and a point characteristic for a second type of defects (here the point $[S_{vc}, W_{vc}]$ representing vacancy clusters). Figure 3 shows that S, W values measured on HPT-deformed Cu samples indeed fall approximately on a straight line. With increasing radial distance from the

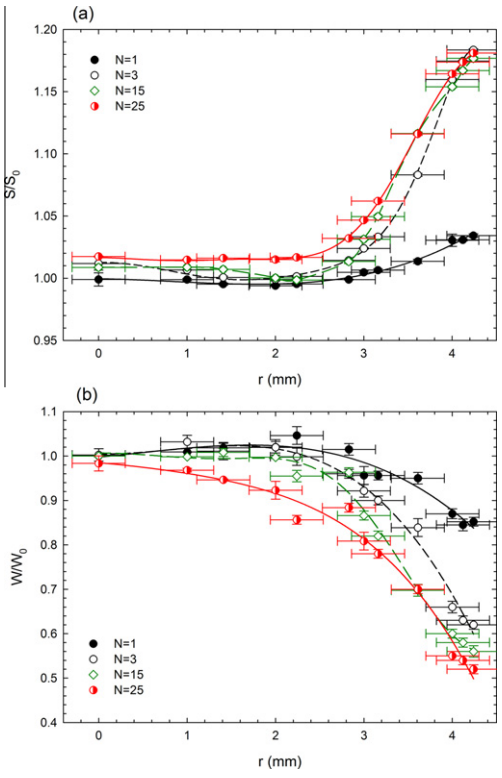

Figure 2. Dependence of (a) the S parameter and (b) the W parameter on the radial distance r from the center of the sample disk. Each point in the figure was calculated as an average of values measured in all nodes of the perpendicular grid at the same distance from the center.

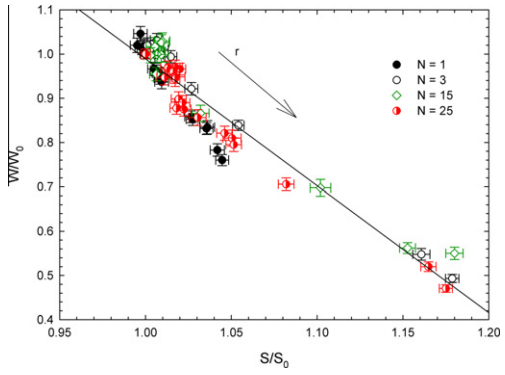

Figure 3. *S–W* plot constructed from the *S* and *W* values measured on a perpendicular grid with incremental spacing of 1.0 mm. With increasing radial distance from the center, the points follow the direction indicated by the arrow. The straight line is a linear fit calculated using all points in the figure.

center, *S* increases and *W* decreases, owing to an increasing fraction of positrons annihilating in vacancy clusters. Hence, the slope of the *S–W* plot is negative. A closer inspection of Figure 3 reveals slight deviations from linearity caused by the increasing size of vacancy clusters with distance from the center. This results not only in an increase in the fraction F_{vc}, but also in an increase in S_{vc} (accompanied by a decrease in W_{vc}). As a consequence, there is a slight change in the slope of the *S–W* plot with increasing distance from the center.

The results presented clearly demonstrate that the DB technique is a valuable tool complementary to widely used HV characterizations. From a technical point of view, the only disadvantage of DB mapping is that it is more time consuming compared with HV characterization. Complete DB mapping of a HPT-deformed sample takes a few days. The main advantages of the DB technique can be summarized as follows.

(i) It is fully non-destructive and enables repetitive measurements of the same sample. This is important, for example, in investigations of the inhomogeneity of thermal recovery of UFG structure which can be performed repetitively on a single sample subjected to subsequent heating steps at various temperatures.

(ii) It provides information about spatial distribution of deformation-induced vacancies which have a relatively low impact on hardness, but strongly influence basic physical processes in UFG materials, e.g., diffusion, phase transitions, etc.

(iii) DB mapping is basically insensitive to surface quality. Therefore, no surface treatment of studied samples is required.

It has to be emphasized that HV and DB mapping are not alternative, but rather complementary techniques providing information about different aspects of microstructure inhomogeneity in HPT-deformed samples. While HV is influenced mainly by the grain size and the dislocation density, DB mapping reflects the spatial distribution of dislocations and also the distribution of deformation-induced vacancies which have a relatively low impact on hardness. The difference between HV and DB mapping can be clearly seen in HPT-deformed Cu. The general trend in HV and *S* is similar, i.e., both increase with increasing radial distance from the center, reflecting increasing defect density and decreasing grain size due to higher imposed strain. However, one can see in Figure 1c that the sample subjected to 25 HPT revolutions is characterized by almost uniform HV, while Figure 1d shows that the *S* parameter in this sample remains significantly higher at the periphery compared with the center. This difference is mainly due to vacancy clusters, which are substantially bigger at the periphery than in the center owing to the higher concentration of deformation-induced vacancies.

In summary, DB mapping using line-shape parameters was successfully employed for characterization of defect distribution in HPT-deformed Cu. It was found that the *S* parameter strongly increases with the radial distance from the center, indicating increasing concentration of defects. Although HV mapping showed only a slight difference between the center and the periphery in the sample subjected to 25 HPT revolutions, DB mapping revealed that lateral distribution of defects is far from being uniform.

This work was supported by the Academy of Science of Czech Republic (Projects Nos. KAN300100801 and IAA101120803) and by the Ministry of Education, Youths and Sports of the Czech Republic through research plan No. MSM 0021620834.

[1] A.P. Zhilyaev, T.G. Langdon, Prog. Mater. Sci. 53 (2008) 893.
[2] Z. Horita, T.G. Langdon, Mater. Sci. Eng., A 410–411 (2005) 422.
[3] J. Čížek, M. Janeček, O. Srba, R. Kužel, Z. Barnovská, I. Procházka, S. Dobatkin, Acta Mater. 59 (2011) 2322.
[4] A.P. Zhilyaev, G.V. Nurislamova, B.K. Kim, M.D. Baro, J.A. Szpunar, T.G. Langdon, Acta Mater. 51 (2003) 753.
[5] A.P. Zhilyaev, K. Oh-ishi, T.G. Langdon, T.R. McNelley, Mater. Sci. Eng., A 410–411 (2005) 277.
[6] Y. Estrin, A. Molotnikov, C.H.J. Davies, R.J. Lapovok, J. Mech. Phys. Solids 56 (2008) 1186.
[7] Ch. Xu, Z. Horita, T.G. Langdon, Acta Mater. 55 (2007) 203.
[8] M. Kawasaki, R.B. Figueiredo, T.G. Langdon, Acta Mater. 59 (2011) 308.
[9] A. Hohenwarter, A. Bachmaier, B. Gludovatz, S. Scheriau, R. Pippan, Int. J. Mater. Res. 100 (2009) 1653.
[10] P. Hautojärvi, in: P. Hautojärvi (Ed.), Positrons in Solids, Springer, Berlin, 1979, p. 1.